Analytical approach to level delocalization and line shifts in finite temperature dense plasmas

X. Li, F.B. Rosmej

Available online at www.sciencedirect.com
ScienceDirect
Physics Letters A 00 (2020) 1–7
Lett. Alogo
Physics Letters A

Analytical approach to level delocalization and line shifts in finite temperature dense plasmas

X. Li[1], F.B. Rosmej[2,3,4,5]

[1]*State Key Laboratory of High Field Laser Physics, Shanghai Institute of Optics & Fine Mechanics, Shanghai 201800, P. R. China*

[2]*Sorbonne University, Faculty of Science and Engineering, UMR 7605, case 128, 4 Place Jussieu, F-75252 Paris Cedex 05 France*

[3]*LULI, Ecole Polytechnique, CEA, CNRS, Laboratoire pour l'Utilisation des Lasers Intenses, Physique Atomique dans les Plasmas Denses, F-91128 Palaiseau, France*

[4]*Moscow Institute of Physics and Technology - MIPT, Institutskii per. 9, Dolgoprudnyi 141700, Russia*

[5]*National Research Nuclear University MEPhI (Moscow Engineering Physics Institute), 115409 Moscow, Kashirskoe sh.31, Russia*

Abstract

X-ray line shifts and delocalization of levels of He-like ions are studied within the framework of the self-consistent multi-configuration relativistic finite temperature ion sphere model. A set of analytical equations for an N-electron bound atomic system to determine X-ray line shifts and level delocalization is proposed that provides very good agreement with numerical calculations, newly high precision line shift measurements of the $1s3p\ ^1P_1 - 1s^2\ ^1S_0\ He_\beta$ transition in Cl^{15+} and the $1s3p\ ^1P_1$-level delocalization in Al^{11+}. We re-analyzed the recently claimed discrepancy between the predictions from the ion sphere model, analytical approaches and the data. The analytical b-potential approach that imitates lattice effects via a perturbation of the free electron distribution in the in sphere is developed and contrasted with currently unexplained line shift measurements of the $1s2p\ ^1P_1 - 1s^2\ ^1S_0\ He_\alpha$ transition in Al^{11+}.

Keywords: Atomic structure, ionization potential depression, finite temperature ion sphere model, laser produced plasmas, X-ray spectroscopy

1. Introduction

The atomic populations are the fundamental quantity for various different disciplines in science and applications, like e.g. the equation of state in thermodynamics, absorption, emission and scattering properties of matter, lasing, radiation transport, radiative cooling and energy loss, diagnostic and spectroscopy employing the radiative properties of matter, astrophysics, planetary science, radiation sources, fusion science [1, 2, 3, 4, 5, 6, 7, 8, 9, 10, 11, 12, 13, 14, 15, 16, 17]. In a low-density environment, where atoms and ions are essentially free, atomic population kinetics of gases and plasmas has been very successful in many different scientific and technical disciplines. As density increases, the free atom model breaks down resulting in a perturbation of the atomic energy levels. The perturbation of atomic levels manifests itself essentially in a broadening and a shift. These perturbations can be observed in high-resolution spectroscopic experiments via the analysis of the line broadening, the line shift and the disappearance of the line emission (corresponding to the ionization potential depression IPD of the upper level). The IPD is of great interest for applications in thermodynamics and also for the understanding of the various radiative properties (emission, absorption, scattering). Since decades, the working horse in dense plasma atomic physics has been a plasma screening potential that acts as a perturber for the free atom Hamiltonian. The screening potential is induced by the charged particle distribution around the ions in plasmas and is rather complex as it involves microfield fluctuations of correlated charged particles. Among a large variety of approaches, the Debye model [18, 7, 19], the Ecker-Kröll model [20], the ion sphere model [21, 7], the Stewart-Pyatt model [22], the Atomic-Solid-Plasma model [23] and the Thomas-Fermi model [24, 25, 26, 7] have widely been applied and made important contributions in the field.

Of particular interest in dense plasma atomic physics is the self-consistent finite temperature ion sphere SCFTIS model: it allows to combine dense plasma effects in a very general manner [7] with the numerical solution of the Schrödinger or Dirac

Email address: xiangdong_li@siom.ac.cn, frank.rosmej@sorbonne-universite.fr (X. Li[1], F.B. Rosmej[2,3,4,5])

equation and allows reaching spectroscopic precision. It is therefore well suited to compare simulations with the data that are obtained in the overwhelming number of cases by spectroscopic methods. Recent measurements have questioned our understanding in the precision of the Multi-Configuration-Dirac-Fock Self-Consistent Finite Temperature Ion Sphere model MCDF-SCFTIS [7, 27, 28]: it was claimed [29] that measured line shift values are significantly smaller than predictions from the self-consistent-field ion-sphere model. However, later numerical analysis showed [30, 31, 32, 33] that excellent agreement with the finite temperature ion sphere model, the arbitrary perturbation potential method APPM [34], the analytical b-parameter potential method [32] and the data is obtained.

In this letter we report on a critical analysis of recent high-resolution spectroscopic data on X-ray line shift measurements [29] and analytical approximations of numerical solutions. We develop a 4^{th}-order analytical approximation of the arbitrary perturbation potential method APPM [34] and demonstrate excellent agreement with the present MCDF - SCFTIS calculations and the data. The analytical approach is generalized for an N-bound-electron system and its total energy shift that is expressed in terms of electron temperature, electron density, principal and orbital quantum number of core bound and optical electrons (described with scaled H-like matrix elements). This analytical approach has spectroscopic precision and is successfully applied to the analysis of line shifts and orbital delocalizations. Its simplicity allows implementation in complex integrated simulations in high energy density physics.

Finally, we develop an analytical solution of an N-electron bound system for the b-parameter potential proposed recently [32] and discuss the results with currently unexplained line shift measurements of the $1s2p\,^1P_1 - 1s^2\,^1S_0$ He_α transition in Al^{11+} [35].

2. X-ray spectroscopic data versus Self-Consistent Finite Temperature Ion Sphere model

The Multi-Configuration-Dirac-Fock Self-Consistent Finite Temperature Ion Sphere model assumes that the dense plasma is composed of ion spheres and solves self-consistently the N-bound electron Dirac-Hamiltonian together with the Poisson equation determined by the free electron plasma density $n_f(r)$ and the bound electron density $n_b(r)$ inside the ion sphere and the nuclear charge Z_n. Each ion-sphere contains one nucleus at the center and numbers N_f and N_b of free and bound electrons, respectively to keep the ion sphere neutral, i.e. $Z_n - N_f - N_b = 0$ or equivalent $Z_n - N_b = \frac{4\pi}{3} R^3 n_e$, where R is the ion sphere radius and n_e is the average plasma free electron density in the ion sphere. The bound electron density is given by

$$n_b(r) = \frac{1}{4\pi} \sum_{j=1}^{N} q_j \left[P_j^2(r) + Q_j^2(r) \right]. \qquad (1)$$

where N is the number of bound electrons, q_j is the number of electrons in the subshell j, and $P_j(r)$ and $Q_j(r)$ are the radial wave functions of the large and small components of orbit j, respectively. More details are described in [7, 27, 28, 36].

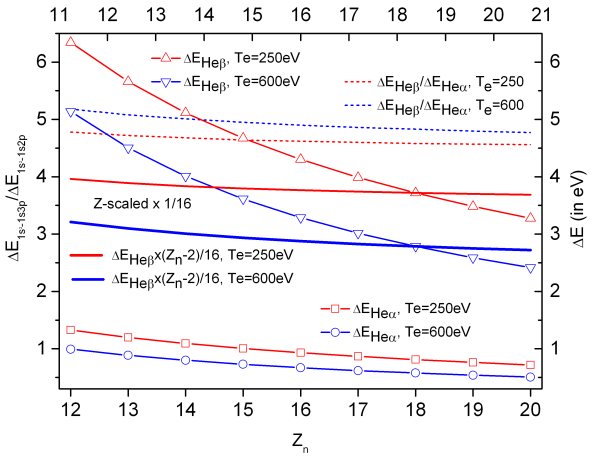

Figure 1. He_β and He_α line shifts for different ions and electron temperatures and fixed electron density $n_e = 3\times10^{23} cm^{-3}$ obtained from the present MCDF-SCFTIS calculations. Also shown are the ratios between the He_β and He_α line shifts and the Z-scaled line shifts of He_β (multiplied by 1/16 for better demonstration).

The solid curves in Fig. 1 represent the theoretical line shifts of He_β and He_α for different atomic number of He-like ions obtained from the present MCDF-SCFTIS calculations, $n_e = 3 \times 10^{23} cm^{-3}$. It can be seen, that the line shift of the He_β-line is about 5 times larger than those of the He_α-line. Also shown are the ratios of these line shifts (dashed lines): a very weak dependence on atomic number is observed for various electron temperatures. The bold solid blue and red lines (designated as "Z-scaled" in Fig. 1) present the He_β-line shifts for different temperatures in a Z-scaled representation, i.e. $\Delta E_{He\beta} \times (Z_n - N_b)$ (note, that for better demonstration in the same figure the scaled results have been divided by a factor of 16). It can likewise be seen, that the dependence on atomic number is also very weak for the scaled shifts. The weak Z-dependence of the scaled shifts is related to parameter cases of hot dense plasmas where the first two positive terms in the APPM [34] are dominant over the negative terms. Numerical calculations for different densities and temperatures indicate similar weak dependences. A comparison of the measured line shifts of the He_β line for a suitable atomic element and different plasma parameters constitutes therefore a relevant test for the MCDF-SCFTIS model that is considered below.

Figure 2 compares the present MCDF-SCFTIS model calculations (red and green crosses, connected with dashed lines) with the measurements (open and solid circles) of the He_β line shifts of Cl^{15+} of [29]. As can be seen the present MCDF-SCFTIS calculations are in excellent agreement with the measurements. Also indicated in the figure are the results from the average ion sphere model [30] (pink solid circles connected with solid line) that provide systematically higher line shift values. Note, that the average atom ISM does not include multi configuration and intermediate coupling effects as does the present MCDF-SCFTIS model, more details are described in [28]. Within the large experimental error bars, we can therefore confirm the

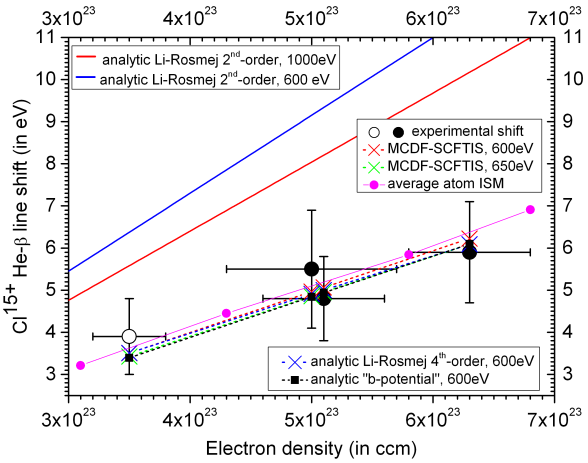

Figure 2. Comparison of the present MCDF-SCFTIS calculations (red and green crosses, connected with dashed lines) for the line shift of the He_β line of Cl^{15+}, the present analytical model (solid black square, connected with dashed line) and the spectroscopic data (open and solid black circles) of [29]. Also shown in the figure our present results employing the analytical model of [36] (4^{th}-order blue crosses, 2^{nd}-order solid blue and red lines) and the average atom ion sphere model ISM from [30] (pink solid circles, connected with solid line).

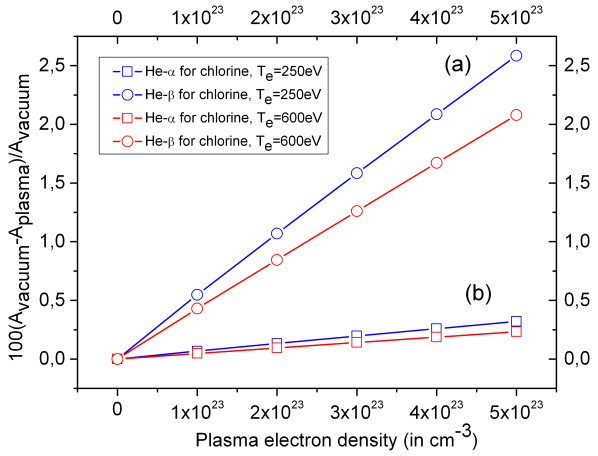

Figure 3. Relative changes of the spontaneous transition probabilities of He_α andHe_β of Cl^{15+} calculated from the present MCDF-SCFTIS model for different densities and temperatures.

statements made in [30, 33] that the measured red shifts show very good agreement with the predictions of the finite temperature ion sphere model.

Let us now shed more light into the various analytical approximations. Based on the APPM [34] an analytical potential for the electron free energy at finite temperature has been derived in the framework of the ion sphere model at finite temperature. This potential has then been expressed in terms of reduced matrix elements $\langle x^{3/2} \rangle$ [34] that does have an analytical representation that is simple and of closed form (it can only be expressed in terms of non-integer Gamma functions [37]). In the work [36] a 2^{nd}-order analytical approximation has been developed that is expressed in terms of simple analytical H-like dipole and quadrupole matrix elements of closed form. Figure 2 shows also the line shifts obtained from this 2^{nd}-order analytical approximation (blue solid and red solid, designated as "Li-Rosmej 2^{nd}-order" in the figure): they are systematically too large compared with the data. The curves with blue crosses (indicated as "Li-Rosmej 4^{th}-order" in Fig. 2) show the results when developing the analytical approach of [36] up to the 4^{th}-order in terms of simple analytic, closed form H-like matrix elements. It can be seen, that the 4^{th}-order analytical approach of [36] provides excellent agreement with the data and also with the numerical calculations. Therefore the differences between the analytical approach of [36] and the data of [29] turn out not to be a conceptual deficiency in the finite temperature ion sphere theory as discussed in [29] but rather to be an effect of the limited precision of the 2^{th}-order approximation of the present MCDF-SCFTIS model compared to the 4^{th}-order series expansion (more details are given in the appendix).

In a dense plasma environment, not only the energy level shift but also the spontaneous transition probabilities are affected. As almost all experimental data for line shifts are obtained by spectroscopic measurements of line intensities in dependence of the frequency, possible perturbation of the Einstein spontaneous transition probabilities A due to the dense plasma environment are also of interest. Fig. 3 shows the relative changes of the transition probabilities as obtained from the present MCDF-SCFTIS model. It can easily be seen, that the relative changes for the He_α-line of Cl^{15+} are not important for the present analysis: much below one percent even for near solid densities. Likewise, also the He_β-line is only affected up to a few percent. Therefore, changes in transition probabilities due to dense plasma effects are negligible for the present analysis and discussion of X-ray line shifts of the He-like Cl^{15+} ions in hot near solid density plasmas.

Let us now apply the MCDF-SCFTIS model to the study of the $1s3p\ ^1P_1$-level delocalization in Al^{11+} as measured in [38]: At $n_e = 2.0 - 2.5 \times 10^{24} cm^{-3}$ and $kT_e = 700eV$ the He_β-line of Al^{11+} is not observed, while at $n_e = 8.6 - 11 \times 10^{23} cm^{-3}$ and $kT_e = 700eV$ the He_β-line is clearly observed. For these parameters, the present MCDF-SCFTIS model calculations provide ionization potential depression values of $196eV - 205eV$ and $158eV - 169eV$, respectively. The analytical model of [36] in 4^{th}-order expansion (see also appendix) provides $198eV - 210eV$ and $157eV - 169eV$, respectively and is therefore in very good agreement with the numerical calculations of level delocalizations too. Because the free atom ionization potential of the $1s3p\ ^1P_1$-level is $220eV$ (as calculated from our MCDF-SCFTIS model) we conclude that He_β should not be observed if the ionization potential depression IPD reaches the value of the free atom ionization potential. As the β-line widths due to the Stark effect are of the order of $50eV$ (Stark broadening calculations show that the FWHM of He_β at $300eV$ and $n_e = 1 \times 10^{23} cm^{-3}$ is about $15eV$ while at $n_e = 1 \times 10^{24} cm^{-3}$ the

FMHM is about $60eV$), the He_β-line should not be observed for the highest densities while for the lower ones He_β should be observed. This is in rather good agreement with the experimental observations.

3. Analytical formulas for the total energy shift of an N-bound electron system

Self-consistent numerical calculations of the MCDF and the Poisson equations are not very convenient neither for dense plasma atomic physics studies nor for integrated simulations in high-energy density physics. We therefore develop a set of analytical closed form equations for a perturbation potential in atomic physics calculations that has spectroscopic precision (line shifts) and allows precision predictions of level delocalization. For these purposes we employ a free electron plasma screening potential of the form [32]

$$\phi_f(r) \approx \frac{N_f}{R}\left[1 + \frac{1}{x-1} - \frac{1}{x-1}\left(\frac{r}{R}\right)^{x-1}\right], \tag{2}$$

where

$$x = 3 - \frac{b\cdot e}{\pi}\sqrt{\frac{N_f}{RT_e}} \tag{3}$$

where R is the ion sphere radius. The free electron distribution $P_f(r)$ is assumed to have the functional dependence according

$$P_f(r) = \frac{N_f}{R^x}\cdot r^x \tag{4}$$

that is consistent with the limit of the Uniform Electron Gas Model UEGM where $x = 3$. b is a parameter that characterizes the self-consistent electron distribution in the ion sphere, e.g. for a Maxwellian electron distribution the MCDF-SCFTIS simulations are matched with $b \approx 2$, while IPD values of near solid density matter could be described with $b \approx 4$ [32]. We note, that approximation (3) is of very good quality if $N_f e^2 \le RT_e$.

Employing first order perturbation theory we find for the energy shift of the N-electron system

$$\begin{aligned} E_p &= \left\langle \Psi_0(r_1,...,r_N)\left|\sum_{i=1}^{N}\phi_f(r_i)\right|\Psi_0(r_1,...,r_N)\right\rangle \\ &= \sum_{i=1}^{N}\frac{N_f}{R}\left[1 + \frac{1}{x-1} - \frac{1}{x-1}\frac{1}{R^{x-1}}\left\langle r_i^{x-1}\right\rangle\right], \end{aligned} \tag{5}$$

where $\left\langle r_i^{x-1}\right\rangle$ is the mean value of r^{x-1} for the i^{th} bound electron. E_p can be calculated analytically if $\left\langle r_i^{x-1}\right\rangle$ has an analytical solution. For H-like ions $\left\langle r^\beta\right\rangle$ can be expressed by the Gamma function Γ for any real β [37]:

$$\left\langle n,l\left|r^\beta\right|n,l\right\rangle = (-1)^{n-l-1}\left(\frac{n}{2\cdot Z}\right)^\beta\frac{1}{2n}\times \sum_{i=0}^{n-l-1}\frac{\zeta(i)\times\Gamma(2l+3+i+\beta)\Gamma(2+i+\beta)}{\Gamma(2l+2+i)\Gamma(n-l-i)\Gamma(l+3-n+i+\beta)}, \tag{6}$$

$$\zeta(i) = \frac{(-1)^i}{\Gamma(i+1)}, \tag{7}$$

where $\beta = x-1$ and $Z = Z^{eff}$ (if the hydrogen-like approach is used for the N bound-electron system). The Gamma-function itself has no analytical closed form solution but can easily be evaluated, e.g. with the method of P. Godfrey [39]. Therefore, the total energy shift for the N bound-electron system can approximated by the expression

$$E_p = \sum_{i=1}^{N}\frac{N_f}{R}\left[1 + \frac{1}{x-1} - \frac{1}{x-1}\frac{1}{R^{x-1}}\left\langle r_i^{x-1}\right\rangle\right], \tag{8}$$

where

$$\left\langle r_i^{x-1}\right\rangle = (-1)^{n-l-1}\left(\frac{n}{2\cdot Z_i^{eff}}\right)^{x-1}\frac{1}{2n}\times \sum_{i=0}^{n-l-1}\frac{\zeta(i)\times\Gamma(2l+3+i+x-1)\Gamma(2+i+x-1)}{\Gamma(2l+2+i)\Gamma(n-l-i)\Gamma(l+3-n+i+x-1)}. \tag{9}$$

Z_i^{eff} is the effective nuclear charge for the i^{th} bound electron and (n,l) are the principle and angular quantum numbers of the i^{th} bound electron. The effective nuclear charge can be calculated by $Z_i^{eff} = n\sqrt{2E_i}$, where E_i is the energy of the i^{th} bound electron. If only one electron is involved in the atomic transition, the corresponding spectral shift ΔE_{shift} can be easily calculated by the difference of the energy shift between the two orbits i and j involved, i.e.

$$\Delta E_{shift} = \left|\frac{N_f}{x-1}\frac{1}{R^x}\left(\left\langle r_j^{x-1}\right\rangle - \left\langle r_i^{x-1}\right\rangle\right)\right| \tag{10}$$

Fig. 2 presents also the analytical approximation of Eq. (10) (solid black squares, connected with dashed line, $b = 2$) that demonstrates very good agreement with the numerical calculations and the data.

Concerning the $1s3p\ ^1P_1$-level delocalization in Al^{11+} at $n_e = 2.0 - 2.5\times10^{24}cm^{-3}$, $kT_e = 700eV$ and $n_e = 8.6 - 11\times10^{23}cm^{-3}$, $kT_e = 700eV$ we obtain (with $b = 2$) $201eV - 212eV$ and $159eV - 171eV$, respectively being in very good agreement with the numerical calculations. This proofs that the analytical potential of eq. (2) has a good spectroscopic precision and therefore considerably facilitates dense plasma atomic structure calculations (because no self-consistent approach with the Poisson equation has to be invoked).

4. Discussion of the analytical b4-potential

Figure 4 shows the line shift measurements of the $1s2p\ ^1P_1 - 1s^2\ ^1S_0$ He_α transition in Al^{11+} [35]. It can clearly be seen, that the MCDF-SCFTIS simulations show much too small values up to a factor of 2.5 for the highest densities measured. The same holds true for the 4^{th}-order analytical expression as well as for the analytical potential method with $b = 2$ that are very close to the MCDF-SCFTIS simulations. Also indicated in the figure are the results from the average ion sphere model [40] (pink solid circles, connected with solid line) that likewise show systematically much to small values compared to the measurements. Therefore, the line shift measurements of the $1s2p\ ^1P_1 - 1s^2\ ^1S_0$ He_α transition in Al^{11+} [35] remained unexplained up to present days.

It has been, however, demonstrated by [32] that the analytical potential of Eq. (2) with b=4 allows to match well the ionization potential measurements of solid density aluminum performed by femtosecond XFEL irradiation of the solid sample as does the Atomic-Solid-Plasma ASP model [23], while MCDF-SCFTIS simulations, the b2-potential (i.e. Eq. (2) with $b = 2$), the Ecker-Kröll model [20] (for discussion of the original and modified Ecker-Kröll model and its confusion in the literature see [23]), and the Stewart-Pyatt model [22] failed. These observations suggests, to use the b4-potential (i.e. Eq. (2) with $b = 4$) to investigate the line shift measurements of [35] that have also been performed near solid densities. The blue dots (connected with blue line) in Fig. 4 show the corresponding b4-potential line shift predictions while the blue dashed line includes the apparent line shifts of [35] (note that the apparent shifts have been defined as shift contributions other than plasma potential shifts, e.g. overlapping satellite contributions, for further discussion see [35]). The figure demonstrates excellent agreement of the b4-potential simulations with the data.

Could Fermi-Dirac effects in the free electron distribution be important ? This is unlikely, because the Fermi energy for the highest densities shown in Fig. 4 is $\epsilon_F \approx 23eV$ while the electron temperature is $kT_e \approx 300eV$, i.e. $\epsilon_F \ll kT_e$. Therefore the chemical potential is close to its asymptotic Maxwellian value of $\mu = -1.5 \cdot kT_e \cdot ln[(m_e kT_e/2\pi\hbar^2 n_e^{2/3}]$. It is therefore suspected that the b4-potential might "imitate" lattice effects for the ionization potential depression and line shifts but a rigorous justification is still missing. We also note that line shift measurements of He_α are rather complex for the reasons discussed in [23] and it appears helpful in view of the present discussion to have line shift measurements like those of [35] available for different low-Z-elements like, e.g. Na, Mg and Si.

5. Conclusion

We have demonstrated that Multi-Configuration-Dirac-Fock Self-Consistent-Finite-Temperature-Ion-Sphere model calculations (MCDF-SCFTIS) and their analytical approximations are in excellent agreement with the data. Recent claims [29] of significant discrepancies between the line shifts of $1s3p\ ^1P_1 - 1s^2\ ^1S_0$ He_β in Cl^{15+} and the analytical 2^{nd}-order approximation of the ion sphere theory turned out not to be a conceptual deficiency in the ion sphere theory but rather to be an effect of the limited precision of the 2^{nd}-order compared to the 4^{th}-order series expansion.

Based on an analytical free plasma electron screening potential we derived a general analytical closed form expression (the "b-potential") for the ionization potential depression and line shift of an N-electron bound atomic system that is expressed only in terms of electron density, electron temperature, energies, principal and orbital quantum numbers. Comparisons with numerical calculations demonstrate very good agreement with the analytical N-electron approach over a wide range of plasma parameters. Finally, we discussed perturbations of the free electron distribution in the ion sphere by means of the analytical b-potential method. It was demonstrated, that the MCDF-SCFTIS simulations are well matched by $b \approx 2$ while lattice effects are imitated with $b \approx 4$. We demonstrated, that the b4-potential matches well the line shift measurements $1s2p\ ^1P_1 - 1s^2\ ^1S_0$ He_α in Al^{11+} of [35] that remained unexplained until present days. To what extent the analytical b-potential could imitate lattice effects for $b > 2$ remains an open question.

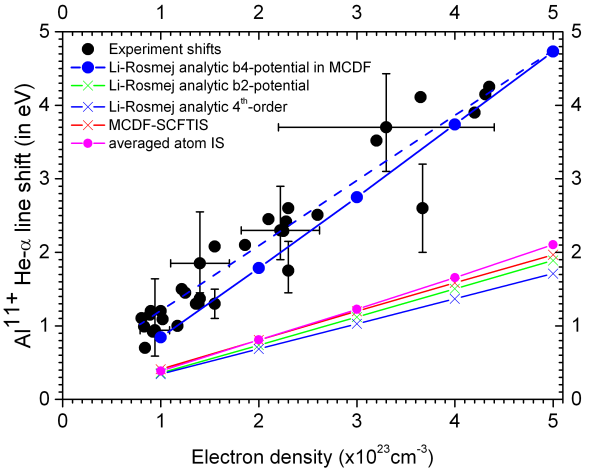

Figure 4. Experimental He_α line shift measurements of Al^{11+} [35] for different densities and their comparisons with different models. The analytic b4-potential provides a good agreement with the data. The dashed blue line shows the b4-potential data that include the apparent shifts [35] and excellent agreement with the measurements is observed. Also shown are the results from the average atom ion sphere model ISM from [40] (pink solid circles). Numerical calculations are carried out for $kT_e = 250eV$.

6. Acknowledgment

This work was supported by the NSFC under Grant No. 11374315, the invited scientist program of CNRS at Ecole Polytechnique (Palaiseau, France), the Formalized Collaboration between the Sorbonne University & MIPT and by NRNU MEPhI in the framework of the Russian Academic Excellence project. Financial support from MIPT, Grant No. 075-02-2019-967 is also greatly acknowledged.

Appendix A. Analytical 4^{th}-order line shift and level delocalization formulas for finite temperature dense plasmas

Below, we provide explicit formulas for the analytical approach proposed in [36] (originally expressed in terms of simple analytical, closed form H-like dipole and quadrupole matrix elements) but in 4^{th}-order approximation:

$$\Delta E_{nl} \approx 2Ry \cdot \frac{Z}{R_0} \cdot \frac{F\left(\left\langle r_i^1\right\rangle, \left\langle r_i^2\right\rangle, \left\langle r_i^3\right\rangle, \left\langle r_i^4\right\rangle\right)}{F\left(R_0, R_0^2, R_0^3, R_0^4\right)} \tag{A.1}$$

$$F(x_1, x_2, x_3, x_4) = \frac{R_0^2}{2} - \frac{x_2}{6} + \frac{4}{3\sqrt{\pi}} \cdot \sqrt{\frac{2RyZ}{kT_e}}$$

$$\times\left(R_0^{3/2} - \frac{2}{5}\left[a_1x_1 + a_2x_2 + a_3x_3 + a_4x_4\right]\right). \quad \text{(A.2)}$$

$Z = Z_n - N_b$ and the sum extends over the number N_b of bound electrons. It should be noted that the representation of the F-function in terms of expectation values $\left\langle r_i^k \right\rangle$, where $k = 1, 2, 3, ...$ is just a convenient way because the integer matrix elements have analytical solutions that are simple, of closed form and only a few matrix elements are requested to achieve good approximations in relevant parameter intervals:

$$\langle r_i \rangle = \frac{1}{2Z_{eff}}\left[3n^2 - l(l+1)\right], \quad \text{(A.3)}$$

$$\left\langle r_i^2 \right\rangle = \frac{n^2}{2Z_{eff}^2}\left[5n^2 + 1 - 3l(l+1)\right], \quad \text{(A.4)}$$

$$\left\langle r_i^3 \right\rangle = \frac{n^2}{8Z_{eff}^3}\left[35n^2(n^2-1) - 30n^2(l+2)(l-1)\right. \quad \text{(A.5)}$$

$$\left. + 3(l+2)(l+1)l(l-1)\right], \quad \text{(A.6)}$$

$$\left\langle r_i^4 \right\rangle = \frac{n^4}{8Z_{eff}^4}\left[63n^4 - 35n^2(2l^2+2l-3)\right. \quad \text{(A.7)}$$

$$\left. + 5l(l+1)(3l^2+3l-10) + 12\right], \quad \text{(A.8)}$$

$$Z_{eff} = n\sqrt{E_{nl}/Ry}, \quad \text{(A.9)}$$

$$R_0 = 1.1723 \times 10^8 \left(Z/n_i \langle Z \rangle\right)^{1/3}. \quad \text{(A.10)}$$

$Ry = 13.606eV$, ΔE_{nl} is the ionization potential depression energy in (eV), E_{nl} is the ionization potential (eV) of the optical electron with principal/orbital quantum numbers nl that move into an effective Coulomb potential with charge Z_{eff}, Z_n is the nuclear charge, $Z = Z_n - N_b$ where N_b is the number of bound electrons, n_i is the ion density in (cm^{-3}), R_0 is the corresponding averaged ion sphere radius in atomic units, $\langle Z \rangle$ is the average charge of the plasma and kT_e is the electron temperature in (eV), $a_1 = 0.77383$, $a_2 = 0.36112$, $a_3 = -0.01605$, $a_4 = 0.000385182$.

Appendix B. Numerical application for He-like argon

Let us apply the set of 4^{th}-order analytical formulas for $kT_e = 600eV$, $n_e = 5 \times 10^{23} cm^{-3}$, $Z_n = 17$, $Z = 15$, $\langle Z \rangle = 15$, $E_{3p} = 386,7eV$, $E_{1s} = 3658eV$: $\Delta E_{3p} = 169.44eV$, $\Delta E_{1s} = 174.35eV$ and for the He_β-line shift of Cl^{15+} $\Delta E_{1s-3p} = 4.9eV$ being in excellent agreement with the data presented in Fig. 2.

References

[1] R. Loudon, The Quantum Theory of Light, 3rd Edition, Oxford Science Publications, 2000.
[2] R. McWhirter, Spectral Intensities, Plasma Diagnostic Techniques, Academic Press, 1965.
[3] H. R. Griem, Plasma Spectroscopy, McGraw-Hill Book Company, New York, 1964.
[4] H. R. Griem, Spectral Line Broadening by Plasmas, Academic Press, New York and London, 1974.
[5] H. R. Griem, Principles of Plasma Spectroscopy, Cambridge University Press, New York, 1997.
[6] I. Sobelman, L. Vainshtein, Excitation of atomic spectra, Alpha Science International Ltd, Oxford, 2006.
[7] D. Salzmann, Atomic Physics in Hot Plasmas, Oxford University Press, New York, 1988.
[8] V. A. Boiko, A. V. Vinogradov, S. A. Pikuz, I. Y. Skobelev, A. Y. Faenov, X-ray spectroscopy of laser produced plasmas, J. Sov. Laser Research 6 (1985) 82.
[9] C. de Michelis, M. Mattioli, Soft x-ray spectroscopic diagnostics of laboratory plasmas, Nuclear Fusion 21 (1981) 677.
[10] V. Lisitsa, Atoms in Plasmas, Springer, New York, 1994.
[11] L. Bureyeva, V. Lisitsa, Perturbed Atom, Astrophysics and Space Physics Reviews, 2000.
[12] A. Unsöld, Physik der Sternatmosphären, Springer, Berlin, 1955.
[13] D. Mihalas, Stellar Atmospheres, 2nd Edition, W.H. Freeman, San Francisco, 1978.
[14] D. Mihalas, B. Weibel-Mihalas, Foundations of Radiation Hydrodynamics, Dover Publications, Mineola, 1999.
[15] G. Bekefi, Radiation processes in plasmas, John Wiley and Sons, New York, 1966.
[16] R. Drake, High-Energy-Density Physics, Springer, Berlin, 2018.
[17] Y. Zel'dovich, Y. Raizer, Physics of Shock Waves and High-Temperature Hydrodynamic Phenomena, Dover Publications Inc., 2002.
[18] P. Debye, E. Hückel, Zur theorie des elektrolyte. i. gefrierpunktserniedrigung und verwandte erscheinungen, Zeitschrit für Physik 24 (1923) 185.
[19] R. Piron, T. Blenski, Free-energy functional of the debye-hückel model of simple fluids, Phys. Rev. E 94 (2016) 062128.
[20] G. Ecker, W. Kröll, Lowering of the ionization energy for a plasma in thermodynamic equilibrium, Phys. Fluids 6 (1963) 62.
[21] G. Zimmermann, R. Moore, Pressure ionization in laser fusion target simulation, JQSRT 23 (1980) 417.
[22] J. Stewart, K. Pyatt, Lowering of ionization potentials in plasmas, Astrophys. J 144 (1996) 1203.
[23] F. Rosmej, Ionization potential depression in an atomic-solid-plasma picture, Letter J. Phys. B. 51 (2018) 09LT01.
[24] B. S. E.H. Lieb, The thomas-fermi theory of atoms, molecules and solids, Advances in Mathematics 23 (1977) 22.
[25] P. Fromy, C. Deutsch, G. Maynard, Thomas-fermi-like and average atom models for dense and hot matter, Phys. Plasmas 3 (1996) 714.
[26] T. Blenski, B. Cichocki, Variational theroy of average-atom and superconfigurations in quantum plasmas, Phys. Rev. E 75 (2007) 056402.
[27] X. Li, Z. Xu, F. Rosmej, Exchange energy shifts under dense plasma conditions, J. Phys. B: At. Mol. Opt. Phys. 39 (2006) 3373.
[28] X. Li, F. Rosmej, Spin-dependent energy-level crossings in highly charged ions due to dense plasma environment, Phys. Rev. A 82 (2010) 022503.
[29] P. Beiersdorfer, G. Brown, A. McKelvey, R. Shepherd, D. Hoarty, C. Brown, M. Hill, L. Hobbs, S. James, J. Morton, L. WIlson, High-resolution measurements of cl^{+15} line shifts in hot, solid-density plasmas, Phys. Rev. A 100 (2019) 012511.
[30] Z.-B. Chen, Calculation of energies and oscillator strengths of cl^{15+} in hot dense plasmas, JQSRT 237 (2019) 106615.
[31] C. Iglesias, On spectral line shifts from analytic fits to the ion-sphere model potential, HEDP 30 (2019) 41.
[32] X. Li, F. B. Rosmej, V. S. Lisitsa, V. A. Astapenko, An analytical plasma screening potential based on the self-consistent-field ion-sphere model, Physics of Plasmas 26 (2019) 033301.
[33] A. Singh, D. Dawra, M. Dimri, A. Jha, R. Pandey, M. Mohan, Plasma screening effects on the atomic structure of he-like ions embeded in strongly coupled plasma, Physics Letters A 384 (2020) 126369.
[34] F. Rosmej, K. Bennadji, V. Lisitsa, Effect of dense plasmas on exchange-energy shifts in highly charged ions: An alternative approach for arbitrary perturbation potentials, Phys. Rev. A 84 (2011) 032512.
[35] C. Stillman, P. Nilson, S. Ivancic, I. Golovkin, C. Mileham, I. Begishev, D. Froula, Picosecond time-resolved measurements of dense plasma line shifts, Phys. Rev. E 95 (2017) 063204.
[36] X. Li, F. Rosmej, Quantum-number-dependent energy level shifts of ions in dense plasmas: A generalized analytical approach, EPL 99 (2012)

33001.
[37] J. Shertzer, Evaluation of matrix elements $\left\langle n,l\left|r^{\beta}\right|n,l'\right\rangle$ for arbitrary β, Phys. Rev. A 44 (1991) 2832.
[38] D. J. Hoarty, P. Allan, S. F. James, C. R. D. Brown, L. M. R. Hobbs, M. P. Hill, J. O. Harris, J. Morton, M. G. Brookes, R. Shepherd, J. Dunn, H. Chen, E. V. Marley, P. B. H. K. Chung, R. Lee, G. Brown, J. Emig, Observations of the effect of ionization-potential depression in hot dense plasma, PRL 110 (2013) 265003.
[39] W. Press, S. Teukolsky, W. Vetterling, B. Flannery, Numercial Recipes, 3rd Edition, Cambridge University Press, Cambridge, 2007.
[40] Z.-B. Chen, K. Wang, Theoretical study on the line shifts of he-like al^{11+} ion imersed in a dense plasma, Radiation Physics and Chemistry 172 (2020) 108816.